International Journal of Pharmaceutics, 51 (1989) 9–17
Elsevier

IJP 01709

The effect of particle size distribution on dissolution rate and oral absorption

Rebecca J. Hintz and Kevin C. Johnson

Pfizer Central Research, Groton, CT 06340 (U.S.A.)

(Received 25 April 1988)
(Modified version received 16 August 1988)
(Accepted 14 September 1988)

Key words: Particle size distribution; Dissolution rate; Oral absorption; Computer simulation

Summary

A computer method has been devised to describe the theoretical dissolution rate of a polydisperse powder under non-sink conditions based on its percent weight particle size distribution. This method was used to estimate the particle size distribution of drug contained in 3 capsule formulations which differed only in the extent of milling of drug used to make the capsules. These distributions served to demonstrate the effect of milling on dissolution rate and were used to simulate their effect on the amount of drug absorbed orally.

Introduction

According to the Noyes-Whitney equation (1897), the rate of dissolution of a solid is dependent upon its solubility, its concentration in solution at a particular time, its diffusivity, and the surface area of the solid. For a drug of low aqueous solubility, particle size and the resulting surface area could have a significant effect on the rate of dissolution over the time interval during which gastrointestinal absorption occurs, and therefore, affect the bioavailability of the drug. A mixing-tank model for predicting the dissolution rate-controlled oral absorption has been presented in the literature (Dressman and Fleisher, 1986) for a monodisperse powder. This model has been modified to treat a polydisperse powder based on its percent weight particle size distribution. The model was then used to simulate the experimental dissolution rate of a poorly water-soluble drug to demonstrate the effect of milling on effective particle size distribution and the resulting effect on dissolution and absorption rate.

Theory

The equations used by Dressman and Fleisher (1986) are reproduced here, followed by a discussion of how these equations were used to simulate a polydisperse powder. The time-dependent factor to account for the gastrointestinal transit of drug particles has been omitted to emphasize how the model can be extended to handle polydisperse particles without changing the rationale of the original authors. The reader is therefore referred

Correspondence: K.C. Johnson, Pfizer Central Research, Groton, CT 06340, U.S.A.

to the derivation of Dressman and Fleisher as to how the omission can be corrected.

A Noyes-Whitney type expression (1897) can be used to describe the dissolution of a monodisperse powder:

$$-\frac{dX_s}{dt} = \frac{DS}{h}\left(C_s - \frac{X_d}{V}\right) \quad (1)$$

where X_s is the mass of solid drug at any time, D is the drug diffusivity, S is the surface area, C_s is the aqueous solubility of the drug, h is the diffusion layer thickness, X_d is the mass of dissolved drug at any time, and V is the volume of the dissolution medium.

Assuming that the particles are monodisperse spheres, and that the number of particles present initially, N_0, does not change with time, the surface area at any time is given by:

$$S = 4\pi r_t^2 N_0 \quad (2)$$

where r_t is the radius at any time t. N_0 can be estimated by the following expression:

$$N_0 = \frac{X_0}{\rho v_0} = \frac{X_0}{\rho \frac{4}{3}\pi r_0^3} \quad (3)$$

where v_0 is the volume of one particle, ρ is the density of the drug, X_0 is the initial mass of drug, and r_0 is the initial particle radius.

The radius of a particle at any time t is given by:

$$r_t = \left(\frac{3X_s}{4\pi\rho N_0}\right)^{1/3} \quad (4)$$

Combining Eqns. 2, 3 and 4 yields:

$$S = \frac{3X_0^{1/3}X_s^{2/3}}{\rho r_0} \quad (5)$$

Substituting Eqn. 5 into Eqn. 1 yields:

$$-\frac{dX_s}{dt} = \frac{3DX_0^{1/3}X_s^{2/3}}{\rho h r_0}\left(C_s - \frac{X_d}{V}\right) \quad (6)$$

Eqn. 6 now expresses the dissolution rate in terms of the initial dose and particle radius. The rate of change of dissolved drug in the GI tract is given by:

$$-\frac{dX_d}{dt} = k_a X_d - \frac{3DX_0^{1/3}X_s^{2/3}}{\rho h r_0}\left(C_s - \frac{X_d}{V}\right) \quad (7)$$

where k_a is the absorption rate constant. The rate of absorption is given by:

$$\frac{dX_a}{dt} = k_a X_d \quad (8)$$

where X_a is the mass of absorbed drug.

The particle size distribution of a polydisperse powder was then simulated by treating it as i discrete monodisperse fractions covering the range of particle sizes observed microscopically in the actual powder. As a starting point, the light microscope can be used to estimate the percent weight distribution of a powder. Each hypothetical monodisperse fraction will then have an initial mass, X_{0_i} and an initial radius, r_{0_i}, where the sum of initial masses from each monodisperse fraction is equal to the dose.

A computer program was then used to calculate the total amount of solid X_{s_T}, dissolved X_{d_T}, and absorbed drug X_{a_T} from the individual monodisperse fractions X_{s_i}, X_{d_i}, and X_{a_i}, respectively. This program used the Runge-Kutta numerical algorithm with a step size of 1 min. Smaller step sizes result in a more accurate estimation. After each minute, the total amount of drug in solution, X_{d_T}, was calculated by adding up the amount of drug dissolved minus the amount of drug absorbed from each fraction. This value was used to calculate a new concentration gradient $C_s - X_{d_T}/V$ that each monodisperse fraction would dissolve against during the next minute interval. This treatment allowed the accurate simulation of experimental data under non-sink conditions. The program also has an internal error handling subroutine to set X_{s_i} equal to zero when it becomes too small to be estimated by the computer. This allows for disappearance of particle fractions and changing population distributions with time

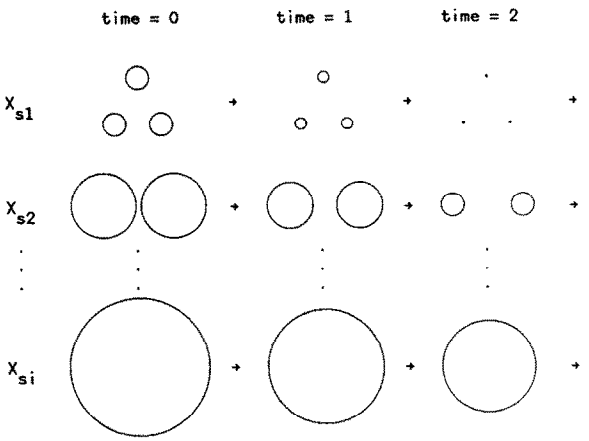

Fig. 1. Schematic representation of the dissolution of a polydisperse powder. For each particle size fraction $i=1$ to n represented in schematic form by rows, the Runge-Kutta method was used to solve Eqns. a–c to calculate the amount of solid drug X_{s_i}, dissolved drug X_{d_i}, and absorbed drug X_{a_i} after a specified time interval. Note that the number of particles in each particle size fraction remained constant with time. After each time interval represented in schematic form by columns, Eqns. d–f were used to calculate the total amount of solid drug X_{s_T}, dissolved drug X_{d_T}, and absorbed drug X_{a_T}. The new value of X_{d_T} after each time interval was used during the next time interval to calculate the concentration gradient and was the same for each particle size fraction during the time interval.

$$\frac{dX_{s_i}}{dt} = -\frac{3DX_{0_i}^{1/3}X_{s_i}^{2/3}}{\rho h r_{0_i}}\left(C_s - \frac{X_{d_T}}{V}\right) \quad (a)$$

$$\frac{dX_{d_i}}{dt} = -k_a X_{d_i} + \frac{3DX_{0_i}^{1/3}X_{s_i}^{2/3}}{\rho h r_{0_i}}\left(C_s - \frac{X_{d_T}}{V}\right) \quad (b)$$

$$\frac{dX_{a_i}}{dt} = k_a X_{d_i} \quad (c)$$

$$X_{s_T} = \sum_{i=1}^{n} X_{s_i} \quad (d)$$

$$X_{d_T} = \sum_{i=1}^{n} X_{d_i} \quad (e)$$

$$X_{a_T} = \sum_{i=1}^{n} X_{a_i} \quad (f)$$

(Leblanc and Fogler, 1987). A schematic representation of this procedure is shown in Fig. 1.

The model used in this analysis assumes that dissolution is controlled by a concentration gradient across an apparent diffusion layer of thickness h. However, h varies with the slip velocity (Harriott, 1962), the relative velocity of the solid to the liquid. In fixed powder beds, for example, h is proportional to the fluid velocity (Carstensen and Dhupar, 1976). For stationary solutions, h is comparable to the radius of the particle (Higuchi and Hiestand, 1963), or equal to the radius for a Sherwood number of 2 (Floyd et al., 1986). The Ranz-Marshall correlation (1952) provides a means of estimating h based on the particle size and slip velocity. For the extreme case of very small particles suspended in a dissolution bath, the slip velocity is negligible (Harriott, 1962), and the stirring rate will have little effect on the rate of dissolution. As the particle size increases, h becomes small relative to r and tends to approach a constant value (Harriott, 1962) since the slip velocity is no longer negligible.

The values of h used to simulate the dissolution profile of a polydisperse powder were estimated in the following manner. A calculated diffusion layer thickness was determined by intrinsic dissolution studies of drug from a compressed disk. For particles whose radius was less than this calculated thickness, the radius of each different particle size was used in Eqn. 6 as the appropriate value for h. For all larger particles, the diffusion layer thickness was set equal to the calculated value. Since the hydrodynamics of a polydisperse powder in a stirred dissolution bath are not known, this is an oversimplification of the real situation. However, accurate simulated dissolution profiles were obtained using this approximation.

Although held constant in the simulations presented in this work, h is a function of time. For small particles, if h is set equal to r_i in Eqn. 4 and substitution is made for N_0:

$$h = r_0\left(\frac{X_s}{X_0}\right)^{1/3} \quad (9)$$

Substituting this relationship into Eqn. 6 gives:

$$-\frac{dX_s}{dt} = \frac{3DX_0^{2/3}X_s^{1/3}}{\rho r_0^2}\left(C_s - \frac{X_d}{V}\right) \quad (10)$$

This results in a faster predicted rate of dissolution than when holding h constant.

Other assumptions used in the simulations are the spherical particle shape and the invariability of this shape with time. However, the present treatment of a polydisperse powder is not limited to any particular shape. For example, if microscopic observation indicated that the particle shape would be better approximated by disks of a thickness w, the following surface area term could be substituted into Eqn. 6:

$$S = \frac{2X_s}{\rho w} + \frac{2X_s^{1/2}X_0^{1/2}}{\rho r_0} \qquad (11)$$

Materials and Methods

Materials

The drug used in this study is an organic compound with a mol. wt. of approximately 320 which does not ionize to any significant extent over the pH range found in the gastrointestinal tract. Its purity is 99.5%. For the purposes of this work, the only important physical properties of the drug are its aqueous solubility, particle size, and diffusivity.

Milling

Three batches of drug were used which differed only in the degree of milling. These batches consisted of the original unmilled drug (Fig. 2A), this batch passed through a Bantam mill (Bantam Mikro-Pulverizer, Pulverizing Machinery, Summit, NJ) fitted with a 0.062 inch Herringbone screen and hammers rotating at 14,000 rpm (Fig. 2B), and the latter milled drug (B) passed again through the Bantam mill fitted with a 0.020 inch Herringbone screen while operating at 14,000 rpm (Fig. 2C). Scanning electron micrographs are shown in Fig. 2.

Apparatus

Dissolution experiments were performed using an Easi-Lift Dissolution Test Station (Hanson Research Corporation, Northridge, CA), a dissolution drive control unit (Hanson), and a solid state temperature control unit (Hanson). Samples were assayed by HPLC using an M-45 pump (Waters Associates, Milford, MA), a Valco injector (Valco

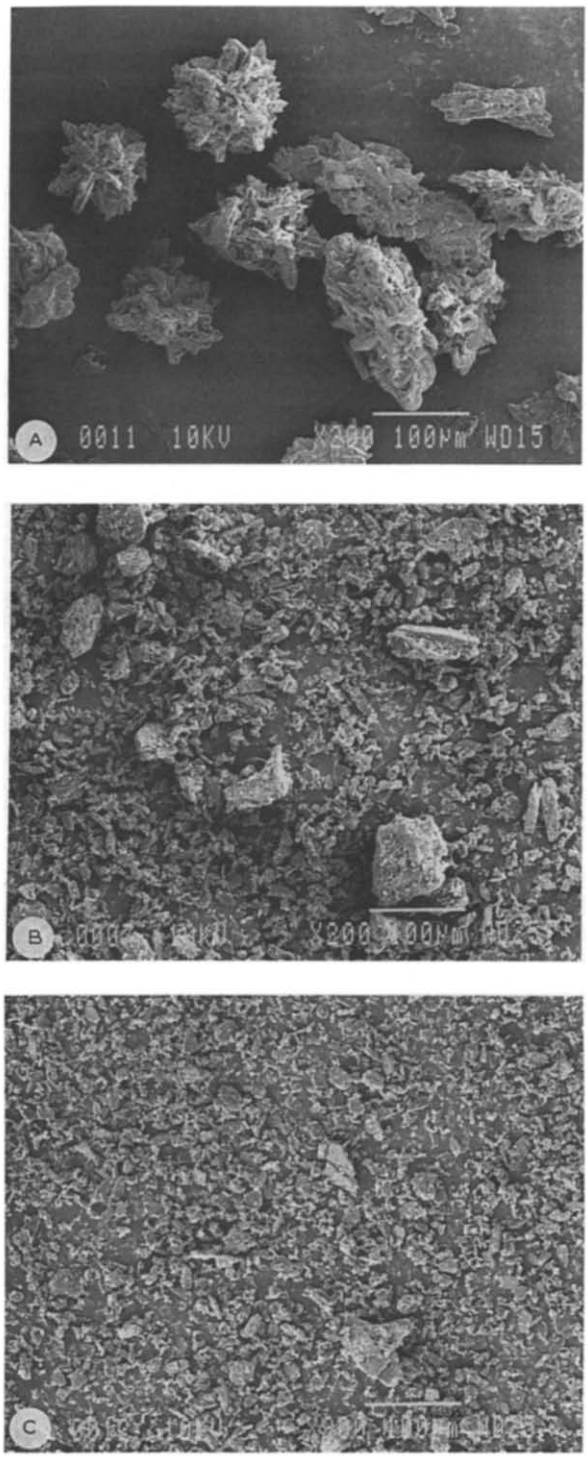

Fig. 2. Scanning electron micrographs of unmilled (A), once-milled (B), and twice-milled (C) drug. SEMs courtesy of J.D. Gagliardo.

Instruments, Houston, TX) fitted with a 10 μl injection loop, a Model 441 absorbance detector (Waters Associates) fitted with a Cadmium lamp (229 λ), and a model 3390A integrator (Hewlett Packard, Avondale, PA). Disks for intrinsic dissolution experiments were compressed into standard tablet dies (Natoli Engineering Co., Chesterfield, MO) using a Model C Carver laboratory press (Fred S. Carver, Menomenee Falls, WI).

Chromatographic conditions

A C-18 column (Microsorb Short-One, Rainin Instrument Co., Woburn, MA) was used with a mobile phase of 75% acetonitrile and 25% water or 0.01 M phosphate buffer adjusted to pH 3 with a flow rate of 1 ml/min.

Solubility

The aqueous solubility of the drug was determined by equilibrating excess drug and water in sealed glass ampules continuously inverted in a 37 °C water bath. After 2 days, the ampules were quickly removed, broken, and their contents immediately filtered (HATF, Millipore, Bedford, MA) and diluted 1 : 1 with mobile phase at ambient temperature. Standards were made by dissolving drug in mobile phase and diluting 1 : 1 with water at ambient temperature. The solubility was determined to be 33 ± 1 μg/ml (95% confidence interval).

Capsules

Three batches of capsules were made differing only in the degree of milling of drug used in the blend. Table 1 shows the capsule blend formula. Capsules were handmade by mixing drug and excipients except magnesium stearate in a bottle for 10 min, passing the blend through a 60 mesh stainless steel screen, blending an additional 10 min, passing the blend through a 60 mesh screen again, adding the magnesium stearate, and blending for 2 min. 5 g of blend were made for each batch of drug with a theoretical potency of 20 mg/500 mg of blend. 3 g of each batch were then used to make 6 no. 0 capsules with a fill weight of 500 mg using a Labocaps capsule-filling apparatus (Adelpi Manufacturing Co., London).

TABLE 1

Capsule blend formulation (mg/capsule)

drug	20.0
80 mesh lactose	422.5
starch 1500	50.0
sodium lauryl sulfate	5.0
magnesium stearate	2.5
	500.0

Intrinsic dissolution

The intrinsic dissolution of drug was studied in 900 ml of filtered, deaerated water at 37 °C with a stirring rate of 25 rpm. Drug was compressed at 2000 psi for 30 s into tablet dies with circular diameters of 1/4 inch, 11/32 inch and 1/2 inch, so that the compressed disk of drug was flush with one face of the die. The other end was covered with parafilm, and the die was placed in the bottom of the dissolution flask with the drug disk facing up. The paddles were lowered to the standard position of 2.5 cm above the bottom of the flask, which positioned them at approximately 3/16 inch from the face of the die. Samples were withdrawn at various time intervals and assayed by HPLC.

Capsule dissolution

Capsule dissolution was then studied in 900 ml of filtered, deaerated water at 37 °C with a stirring rate of 75 rpm. Capsules were anchored using a coil (~ 2 wraps) of copper wire and dropped into the dissolution bath at time zero. Samples were filtered (HATF, Millipore) before being assayed by HPLC.

Particle size distributions

The percent weight particle size distributions of unmilled, once-milled, and twice-milled drug were determined using a Coulter Counter (Model TA, Hialeah, FL) and by the computer method described in the theoretical section.

The electrolyte solution for the Coulter Counter contained 1% NaCl and 1 drop of Tween 20 per liter. After saturating the electrolyte with drug and filtering, samples were dispersed in the electrolyte with approximately 5 s of mild sonication.

Suspended drug was drawn through a 280 μm aperture for 100 s.

Particle size distributions using the computer method were determined in the following manner. The initial mass of drug contained in a capsule (20 mg) was divided into 16 discrete particle size fractions based on a rough estimate of the percent weight particle size distribution. For ease of comparison, the number of fractions and their corresponding particle size were chosen to match the number of ranges and the upper value in each particle size range output from the Coulter Counter, respectively. Using the approximate initial mass, and the appropriate radius and diffusion layer thickness for each particle size fraction, Eqn. 6 was used to calculate the amount of drug that dissolved for each particle size fraction. The Runge-Kutta method with a step size of 1 min was used to solve Eqn. 6. After each minute, the total mass dissolved was calculated. At the appropriate time points, the calculated total mass of dissolved drug was subtracted from the experimental mass of dissolved drug from the dissolution experiment (see Table 2). The differences were then squared and totaled. This process was repeated using a different initial particle size mass distribution until the sum of squares was minimized.

Results and Discussion

The intrinsic dissolution from compressed disks is shown in Fig. 3. Based on the slopes of the lines,

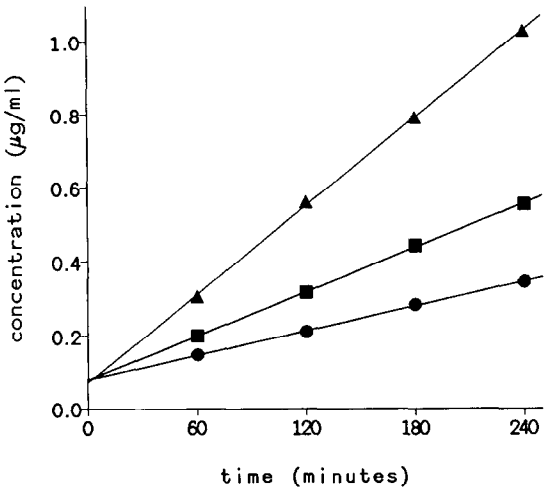

Fig. 3. Intrinsic dissolution of drug from compressed disks of diameter 1/4 inch (circles), 11/32 inch (squares), and 1/2 inch (triangles) in 900 ml of water at 37 ° C.

the intrinsic dissolution rate constant was 0.09 ± 0.01 cm/min, resulting in a calculated diffusion layer thickness of 30 8gmm (Carstensen, 1977). As discussed in the theoretical section, 30 μm was used as the transition particle radius, below which the diffusion layer thickness equaled the radius and above which equaled 30 μm as shown in Fig. 4.

Table 2 lists the percent of drug dissolved for the 3 batches of capsules. This data is also shown

TABLE 2

Capsule dissolution data

Time (min)	Percent drug dissolved		
	A	B	C
15	15.1 ± 1.9 *	45.9 ± 5.5	63.4 ± 2.5
30	22.7 ± 4.7	59.1 ± 6.2	80.5 ± 5.7
45	29.5 ± 1.6	66.8 ± 2.5	87.3 ± 1.9
60	35.1 ± 1.9	72.0 ± 2.2	90.7 ± 3.0
120	49.3 ± 3.6	80.2 ± 1.5	95.2 ± 3.7
180	60.1 ± 6.3	86.1 ± 3.4	96.2 ± 5.9
240	67.5 ± 8.6	88.8 ± 2.3	99.2 ± 1.1

* 95% confidence interval ($n = 3$).

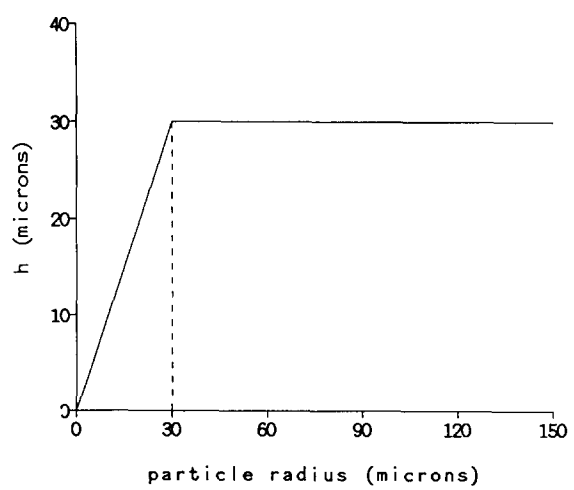

Fig. 4. Diffusion layer thickness h as a function of particle radius.

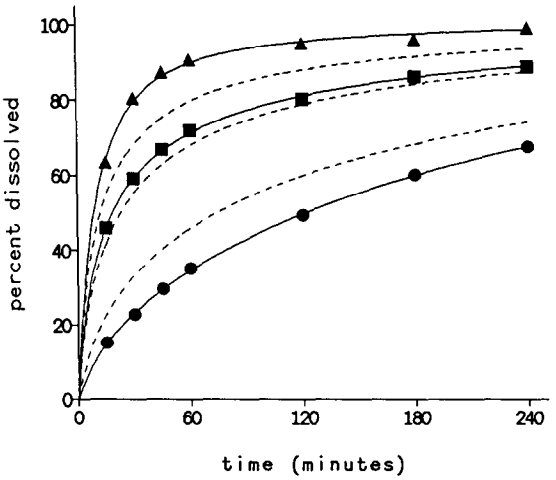

Fig. 5. Dissolution profiles of capsules containing 20 mg of unmilled drug (circles), once-milled drug (squares), and twice-milled drug (triangles) in 900 ml of water at 37 °C. Solid lines represent computer-simulated dissolution profiles based on the particle size weight distributions shown in Fig. 6. Dashed lines represent dissolution profiles based on the Coulter particle size weight distributions shown in Fig. 7.

in Fig. 5 along with theoretical curves generated using the procedure for simulating the dissolution of a polydisperse powder described earlier. These theoretical curves represent a mechanistic fit of the dissolution data based on a particle size weight distribution rather than a simple function such as a polynomial. For this reason, several simulations were generated by changing the particle size weight distribution. The curve with the least squared fit is shown in Fig. 5. Also shown in Fig. 5 are simulated dissolution profiles based on an initial particle size mass distribution as measured by the Coulter Counter. The initial radii used corresponded with the upper values in each particle size range.

The computer-simulated and Coulter-measured particle size weight distributions that were used to generate the curves in Fig. 5 are shown in Figs. 6 and 7, respectively. The range of particle size represented in the distributions agreed with the order of magnitude indicated by scanning electron micrographs of the actual drug samples (see Fig. 2). In our opinion, the computer-simulated and Coulter particle size distributions agree well with

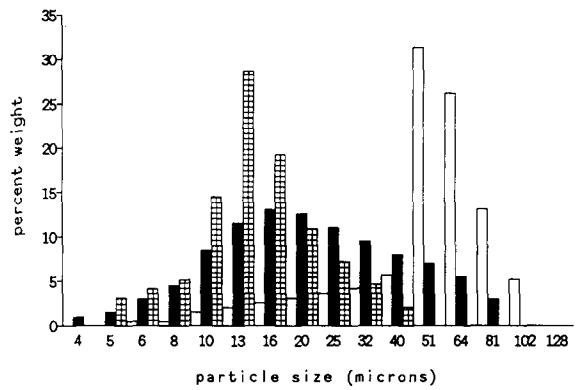

Fig. 6. Computer-estimated particle size weight distributions of unmilled drug (open bars), once-milled drug (solid bars), and twice-milled drug (screened bars).

each other and support the assumptions made in modeling the dissolution of a polydisperse powder.

The simulated distributions should be viewed as effective particle size weight distributions since the analysis was done assuming that the particles were perfect spheres. In essence, the present modeling of dissolution has translated the effect of particle shape, size, distribution, and hydrodynamics into those of perfect spheres. In theory, if the hydrodynamics in vitro are the same as in vivo, then these particle size distributions could be used to predict the dissolution rate in the volume of fluid that exists in the GI tract. Future research into devising an in vitro dissolution test that closely approximates the hydrodynamics in vivo would

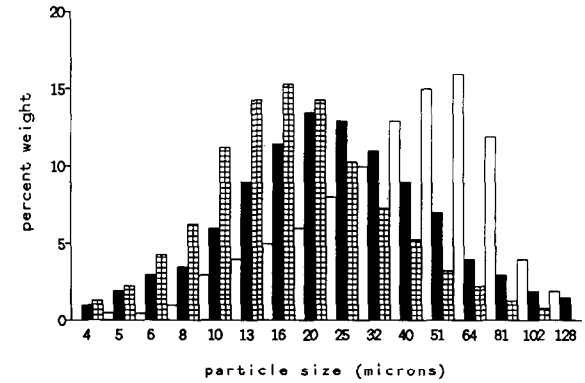

Fig. 7. Particle size distributions of unmilled drug (open bars), once-milled drug (solid bars), and twice-milled drug (screened bars) measured by the Coulter Counter.

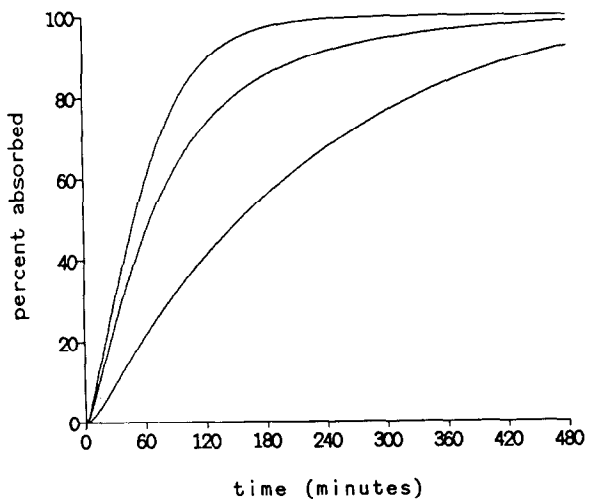

Fig. 8. Computer-simulated percent of dose absorbed for 20 mg capsules of unmilled drug, once-milled drug, and twice-milled drug from bottom to top, respectively, based on the particle size weight distributions shown in Fig. 6.

yield an effective particle size distribution that would improve the accuracy of in vivo simulations.

The particle size distributions in Fig. 6 were then used to simulate the amount of drug absorbed by changing the volume of the dissolution medium from 900 ml to a more physiological volume of 250 ml for the gastrointestinal tract (Dressman et al., 1985) and by incorporating an absorption rate constant of 0.035 min^{-1} into Eqns. 7 and 8. The absorption rate constant was estimated by rat intestinal perfusion experiments using the method of Amidon et al. (1980). Fig. 8 shows the simulated percent of dose absorbed and demonstrates the importance of the particle size distribution on the amount of drug absorbed for a dissolution rate controlled process, i.e. when the drug is poorly soluble.

The total amount of dissolved drug X_{d_T} is an important parameter since its proper calculation allows for simulations under non-sink conditions. In the model used here, each hypothetical monodisperse powder dissolves at a rate based on its own mass and surface area but against the gradient of the same total concentration of drug in solution. In a simulation of in vitro dissolution, the rate of dissolution for all particle sizes slows down as the total amount of dissolved drug approaches saturation. In the in vivo case, the rate of dissolution of some particles may actually increase with time because the total amount of dissolved drug eventually approaches zero due to absorption. The model successfully accounts for both cases. Fig. 9 shows the total amount of dissolved drug for both in vitro and in vivo simulations by using the same dissolution volume.

This model offers an improvement to that of Dressman and Fleisher (1986) by simulating the dissolution of a polydisperse powder. It can also be used in conjunction with pharmacokinetic models to more accurately estimate pharmacokinetic parameters. For example, significant error can be introduced in estimating the elimination rate constant from drug plasma data if absorption is still occurring during the terminal phase. The model provides an estimation of when absorption is complete but also enables one to estimate the elimination rate constant when absorption is still occurring because its contribution to the plasma drug concentration versus elimination is taken into account in a mass balance. Fig. 10 shows simulated blood plasma concentrations using the 3 particle size distributions in Fig. 6. These simulations were made by using the model to input the

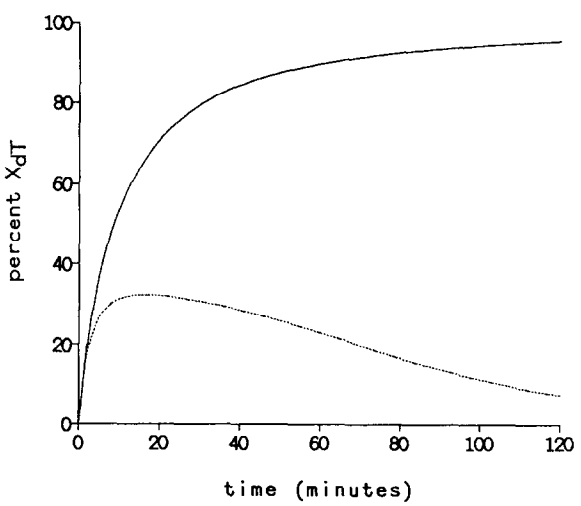

Fig. 9. Total dissolved drug X_{d_T} calculated for a capsule made with twice-milled drug in 900 ml of water (solid line) and in 900 ml with an absorption rate constant of 0.035/min (dotted line).

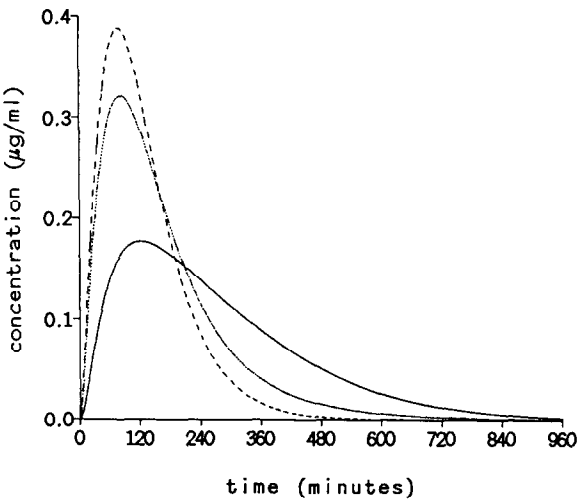

Fig. 10. Simulated blood plasma drug concentration for unmilled (solid line), once-milled drug (dotted line), and twice-milled drug (dashed line). The following parameters were used: dissolution volume 250 ml; absorption rate constant 0.035/min; volume of distribution 20 liter; elimination half-life 46 min.

drug absorption rate into a one-compartment pharmacokinetic model with first-order elimination. The importance of absorption rate based on dissolution rate can be seen as well as the difficulty in estimating the elimination rate constant using traditional techniques such as curve stripping.

In conclusion, a theoretically based method has been developed to describe the dissolution of a polydisperse powder under non-sink conditions. This approach has its greatest utility when applied to poorly water-soluble drugs. Simulation of the dissolution data using this method provides an effective particle size distribution that can be used to identify the most appropriate particle sizing technique with which to simulate dissolution. The hydrodynamic assumptions and the particle shape can also be modified to improve the agreement between simulated and measured particle size distributions. The model can be used in conjunction with pharmacokinetic models as a means of more accurately simulating the absorption of a drug based on its solubility and particle size weight distribution. This would allow a more meaningful interpretation of blood plasma drug concentration data for poorly soluble drugs as well as allowing a more accurate estimation of pharmacokinetic parameters such as the elimination rate constant.

Acknowledgement

We would like to thank Dr. David S. Dresback, Dr. Eugene F. Fiese, and Dr. Timothy A. Hagen for their comments during the preparation of the manuscript.

References

Amidon, G.L., Leesman, G.D. and Elliot, R.L., Improving intestinal absorption of water-insoluble compounds: a membrane metabolism strategy. *J. Pharm. Sci.*, 69 (1980) 1363–1368.

Carstensen, J.T., *Pharmaceutics of Solids and Solid Dosage Forms*, Wiley, New York, 1977, p. 66.

Carstensen, J.T. and Dhupar, K., Dissolution rate equations in column-confined dissolution. *J. Pharm. Sci.*, 65 (1976) 1634–1639.

Dressman, J.B., Amidon, G.L., and Fleisher, D., Absorption potential: estimating the fraction absorbed for orally administered compounds. *J. Pharm. Sci.*, 74 (1985) 588–589.

Dressman, J.B. and Fleisher, D., Mixing-tank model for predicting dissolution rate control of oral absorption. *J. Pharm. Sci.*, 75 (1986) 109–116.

Floyd, S., Choi, K.Y., Taylor, T.W., and Ray, W.H., Polymerization of olefins through heterogeneous catalysis IV. Modeling of heat and mass transfer resistance in the polymer particle boundary layer. *J. Appl. Polymer Sci.*, 31 (1986) 2231–2265.

Harriott, P., Mass transfer to particles. I: Suspended in agitated tanks. *AIChE J.*, 8 (1962) 93–101.

Higuchi, W.I. and Hiestand, E.N., Dissolution rates of finely divided drug powders. I. Effect of a distribution of particle sizes in a diffusion-controlled process. *J. Pharm. Sci.*, 52 (1963) 67–71.

Leblanc, S.E. and Fogler, H.S., Population balance modeling of the dissolution of polydisperse solids: rate limiting regimes. *AIChE J.*, 33 (1987) 54–63.

Noyes, A.A. and Whitney, W.R., The rate of solution of solid substances in their own solutions. *J. Am. Chem. Soc.*, 19 (1987) 930–934.

Ranz, W.E. and Marshall, W.R., Jr., Evaporation from drops. I. *Chem. Eng. Prog.*, 48 (1952) 141–146.